It is seen from our experimental data that the emission band of crystalline neon has a line structure, and the spectrum itself lies in the region of the resonance luminescence of the free neon atom. Special experiments were performed to show that the observed radiation belongs indeed to neon in the crystalline state. The spectra were measured at different condensation rates, at different points of the same crystal and in crystals of different thickness, and at different powers of the exciting electron beam. The spectra were registered immediately after condensation and after storing the samples in vacuum. In all cases, the line structure, the positions of the components in the spectra, and their relative intensities remained unchanged. This means that we have observed the proper luminescence of solid neon.

The structure of the luminescence spectrum is governed by several different factors. The two line pairs 743, 735, and 739.5, 731.5 Å are similar and have a spin-orbit splitting characteristic of the free atom ($\Delta\nu_{so}$ = 1430 cm^{-1}). The first pair practically coincides with the spin-orbit doublet in the gas. The occurrence of two pairs of a spin-orbit doublet is connected, in our opinion, with the splitting of the $^3P_1$ and $^1P_1$ levels in the crystal. This splitting ($\Delta\nu_c$ = 640 cm^{-1}) is the result of a lowering of the luminescence-center symmetry. When the neon atom is excited to a P state with elongated electron orbit, the degeneracy should be lifted as a result of the asymmetrical distortion of the crystal lattice. In order for each of the P terms to split into two, it suffices to lower the point symmetry of the luminescence center locally from octahedral to axial.

The broader maximum near 748 Å is apparently due to the $^3P_2 - {}^1S_0$ transition, which is forbidden in the free atom and has never been observed before in the spectrum of neon. This transition may become allowed in the crystal because of violation of the spherical symmetry. The width of this maximum may be connected with the presence of several unresolved components.

The proximity of the lines in the solid and gaseous phases is the consequence of the low polarizability of the neon atoms.

[1] Y. Frenkel, Phys. Rev. 37, 17, 1276 (1931).
[2] N.G. Basov, O.V. Bogdankevich, V.A. Danilychev, G.N. Kashnikov, et al., ZhETF Pis. Red. 7, 404 (1968) [JETP Lett. 7, 317 (1968)]; J. Luminescence 1, 834 (1970).
[3] J. Jortner, L. Meyer, S.A. Rice, and E.G. Wilson, J. Chem. Phys. 42, 4250 (1965).
[4] R.E. Packard, F. Reif, and C.H. Surko, Phys. Rev. Lett. 25, 1435 (1970).
[5] A.G. Belov, E.V. Savchenko, and I.Ya. Fugol', Fizika kondensirovannogo sostoyaniya (Physics of the Condensed State), Physico-tech. Inst. of Low Temperature, Ukr. Acad. Sci. (Khar'kov), No. 10, 229 (1970).
[6] M. Martin, J. Chem. Phys. 54, 3289 (1971).
[7] T.E. Stewart, G.S. Hurst, T.E. Bortner, J.E. Parks, F.W. Martin, and H. Weidner, JOSA 60, 1290 (1970).

SPECTRA OF PARTICLES AND ANTIPARTICLES IN THE CENTRAL REGION

L.E. Gendenshtein and A.B. Kaidalov
Physico-technical Institute, Ukrainian Academy of Sciences

Submitted 23 July 1972
ZhETF Pis. Red. 16, No. 4, 249 - 253 (20 August 1972)

Interest in the inclusive [1] reactions a + b → c + x has greatly increased of late. Various dynamic models, such as the multiperipheral model (MPM) [2] and the multireggeon model [3], and also an approach based on the use of the

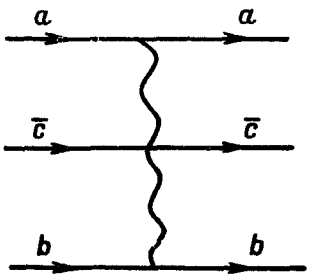

Fig. 1

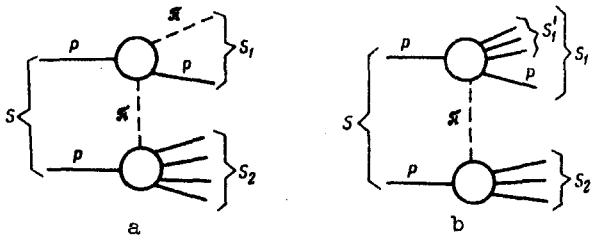

Fig. 2

Regge phenomonology for the amplitudes of the transition $a + b + \bar{c} \to a + b + \bar{c}$ [4, 5] lead to scaling for the inclusive processes at high energies and to a number of interesting predictions concerning the properties of the single-particle spectra.

In the present article we discuss the behavior of the spectra of particles and antiparticles in the central region, i.e., when the variables $x = p_c^{\parallel}/p_a \ll 1$, where $p_c^{\parallel}$ is the longitudinal momentum of particle c. All the models mentioned above lead to asymptotic equality of the spectra of the particles and antiparticles as $x \to 0$. The reason is that the cross section of the inclusive process is expressed in terms of a definite jump of the amplitude of the reaction $a + b + \bar{c} \to a + b + \bar{c}$ [4, 6], which is described by the two-reggeon diagram of Fig. 1 as $s \to \infty$ and $x \to 0$. If $s_{ac} = (p_a + p_c)^2 \simeq [M_c^2 + (p_c^{\perp})^2]/x$ and $s_{bc} = (p_b + p_c)^2 \simeq sx \gg M^2$, then vacuum poles having a definite C-parity predominate, and therefore the vertices cPPc and $\bar{c}PP\bar{c}$ are identical (this statement holds also when allowance is made for the branch cuts connected with the exchange of several vacuum poles).

It seems that an experimental verification of the asymptotic equality is quite important as a check on the applicability of the method of complex angular momenta to the analysis of inclusive reactions. We shall show below that although in pp collisions the yields of p and $\bar{p}$, and also of K^+ and K^-, differ strongly at energies up to 10^3 GeV and $x \sim 0.1 - 0.2$ [7], there is a simple mechanism that explains this difference and makes it possible to describe the spectra.

We consider, for concreteness, the spectra of p and $\bar{p}$ and use the quantity x defined in the laboratory frame. The central region of interest to us is characterized by $x \sim M_p/\sqrt{s}$. Within the framework of the multiperipheral model, as $s \to \infty$, the mechanisms of proton and antiproton production in the central region are identical, and consist of production of baryon-antibaryon pairs in the center of the MPM chain. This indeed explains why the p and $\bar{p}$ spectra are asymptotically equal in the central region in this model.

At the same time, another mechanism for the production of protons with $x \sim M_p/\sqrt{s}$ exists at accelerator energies ($E \sim 10 - 10^3$ GeV/c) and predominates significantly over the mechanism mentioned above. We have in mind the diagrams of Figs. 2a and 2b, where backward elastic (or inelastic) pion-nucleon scattering occurs in the upper block. As $s \to \infty$ and $x \to 0$, the contribution of such diagrams decreases at least like $\sqrt{x}$.

Let us consider first the contribution of the diagram of Fig. 2a to the cross section for the production of protons with $p_{\perp} = 0$. At small x and $s \gg M_p^2$ we have

$$\frac{d^2\sigma}{dpd\Omega} = \frac{p_a x^2}{4\pi^3 M^4} \int_{s_{thr}}^{M^2/x} ds_1 \sigma_{\pi N}^{tot} \frac{d\sigma_1}{d\Omega_1}(s_1) \frac{s_1^2(M^2 - s_1 x)}{s_1 - M^2} \int_{-\infty}^{t_{min}} F(t)\,dt, \qquad (1)$$

where p_a is the momentum of the incident proton, $\sigma_{\pi N}^{tot}$ is the total cross section for pion-nucleon interaction in the lower block, $d\sigma_1/d\Omega_1$ is the sum of the differential cross sections of backward $\pi^{\pm}_0 p$ scattering, $F(t)$ is a function characterizing the dependence on the squared momentum of the virtual pion, and $t_{min} = -[(1 - x)/x](M^2 - s_1 x)$. Since $Ed^3\sigma/d^3p \simeq (xp_a)^{-1} d^2\sigma/dpd\Omega$, formula (1) leads to a scaling-invariant expression for $E(d^3\sigma/d^3p)$.

We shall use for $F(t)$ a parametrization proposed in [9]:

$$F(t) = \begin{cases} 1/(t - \mu^2)^2 & |t| < |t_0| \\ e^{\lambda t'}/(t_0 - \mu^2)^2 & |t| > |t_0|, \quad t' = t - t_0 \end{cases} \qquad (2)$$

i.e., one-pion exchange predominates in the region of small $|t|$, and in the region of large $|t|$ the exponential dependence ensures the peripheral character of the interaction. The dashed curve in Fig. 3 shows the contribution of the diagram of Fig. 2a to $d^2\sigma/dpd\Omega$ at $p_a = 30$ GeV/c if we choose $|t_0| = 0.5$ GeV^2 and $\lambda = 1.75$ GeV^{-2}. The experimental data were taken from [10]. As $x \to 0$ and $s \to \infty$, the main contribution to the integral in (1) is given by the region $s_1 \simeq M^2/x$ and $d^2\sigma/dpd\Omega \propto x^2 d\sigma_1/d\Omega_1(M^2/x)$. Since $d\sigma_1/d\Omega_1 \propto s_1^{2\alpha_N - 1}$ at high energies, the contribution of the backward elastic pion-nucleon scattering to $d^2\sigma dpd\Omega \propto x^{3-2\alpha_N} \simeq x^{3.6}$.

At $s_1 \gtrsim 4$ GeV^2 and $x \lesssim 0.2$, an appreciable contribution to the cross section is made by the backward inelastic proton scattering (Fig. 2b). By estimating this diagram on the basis of experimental data [11] on backward pion-nucleon inelastic scattering, we obtain for the total contribution of both diagrams (2a

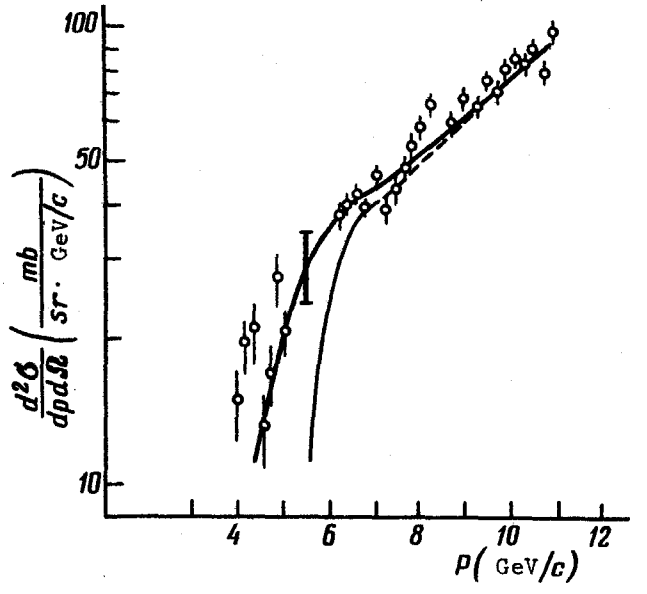

Fig. 3

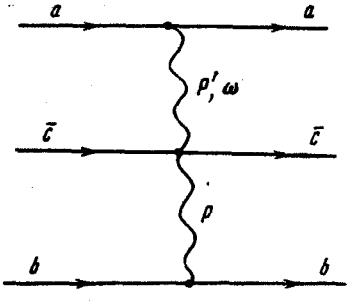

Fig. 4

and 2b) the continuous curve of Fig. 3, which corresponds to the experimental data. Figure 3 shows also the theoretical uncertainty connected with the estimate of the contribution of the inelastic scattering. As $x \to 0$ and $s \to \infty$, the inelastic processes in the upper blocks dominate, with $s_1' \sim s_1 \simeq M^2/x$, where s_1' is the square of the beam mass.

When $s_1' \gg M^2$, the cross section of the inclusive process is connected with the jump of the amplitude corresponding to the diagram of Fig. 4, where exchange of secondary Regge poles x P', ω, etc., for which $\alpha_R(0) \simeq 1/2$, takes place in the upper part of the diagram.

If duality is valid, then the cross section behaves in such a way also at relatively small s_1. We note that according to duality such a mechanism obtains only in the case of proton production, since the $a\bar{c}$ channel for $\bar{p}$ is exotic. The contribution of the diagram 2b to the cross section for the production of protons in the region of small x is quite appreciable and $d^2\sigma/dpd\Omega \propto x^{2-\alpha_R} \simeq x^{3/2}$. Thus, as $s \to \infty$ and $x \to 0$ we obtain for the invariant cross section $Ed^3\sigma/d^3p$ the following expansion:

$$E\frac{d^3\sigma}{d^3p} \simeq C_p + C_R(x^{1/2} + (xs)^{-1/2}) + C_1(x^{2-2\alpha_N} + (xs)^{2\alpha_N - 2}). \qquad (3)$$

(the second terms in the parentheses in (3) describe analogous contributions from the fragmentation of the target), where C_p corresponds to emission of $p\bar{p}$ pairs from the middle of the multiperipheral chain (this term is the same for p and $\bar{p}$), C_1 and C_R are determined by the contributions of diagrams 2a and 2b, respectively, with $C_R \simeq 1/30$, $C_1 \simeq 5C_p$. Therefore the cross section for the production of protons having a momentum p''_{cms} in the c.m.s. of the colliding particles ($x \simeq M/\sqrt{s}$) will decrease all the way to energies $s \sim 10^3$ GeV^2 like $(M/\sqrt{s})^{1/2}$. The yields of $\bar{p}$ in this region can increase somewhat in comparison with those measured at $p_a = 19$ GeV/c [8], for owing to the large mass of the $p\bar{p}$ pair this energy is still relatively low with respect to the $\bar{p}$ production threshold, and the effects connected with the increase of the phase volume can play a noticeable role. We emphasize that in order for the inclusive $\bar{p}$ cross section to reach the asymptotic value C_p connected with the volume by the two vacuum poles in Fig. 1, it is necessary that a large number of pions be produced in addition to the $p\bar{p}$ pair; this is in general not the case at energies $\sim$10 GeV.

A similar situation obtains in the case of K^+ and K^- meson production. The K^- mesons are produced mainly in the center of the MPM chain, whereas the K^+ mesons can be produced, with high probability, jointly with strange baryons in the upper block of the MPM chain.

An experimental verification of these predictions of the multipheripheral model is of considerable interest.

The authors thank A.I. Akhiezer for interest in the work and K.A. Ter-Martirosyan and D.V. Volkov for discussions.

[1] R.P. Feynman, Phys. Rev. Lett. 23, 1415 (1969).
[2] D. Amati, A. Stanghellini, and S. Fubini, Nuovo Cim. 26, 896 (1962).
[3] L. Caneshi and A. Pignotti, Phys. Rev. Lett. 22, 1219 (1969).
[4] A. Mueller, Phys. Rev. D2, 2963 (1970).
[5] V.A. Abramovskii, O.V. Kancheli, and I.D. Mandzhavidze, Yad. Fiz. 13, 1102 (1971) [Sov. J. Nuc. Phys. 13, 630 (1971)].

[6] H. Stapp, Phys. Rev. D3, 3177 (1971).
[7] J. Allaby et al., Preprint CERN 70 - 12 (1970).
[8] L. Ratner el al., Phys. Rev. Lett. 27, 68 (1971).
[9] K.G. Boreskov, A.B. Kaidalov, and L.A. Ponomarev, Paper delivered at Internat. Conf. on High-energy Physics, Oxford, 1972.
[10] E. Anderson et al., Phys. Rev. Lett. 19, 198 (1967).
[11] E. Anderson et al., Phys. Rev. Lett. 22, 102 (1969); 23, 721 (1969); P. Carlson et al., Phys. Lett. 35B, 502 (1970).

E R R A T A

Article by A. Yu. Aleksandrov et al., Vol. 16, No. 4:

On p. 147, lines 17 - 18 from top, read ...Cs_2SbCl_6(B) and $RbSbCl_6 \cdot 2Rb_3SbCl_6$(A).... instead of ... Cs_2SbCl_6(A) and $RbSbCl_6 \cdot 2Rb_3SbCl_6$(B).

On p. 148, lines 16 - 17 from the bottom, read ...$kT_n \sim Vz$... instead of ...$kT_n \sim V_z$...

Article by L. E. Gendenshtein and A. B. Kaidalov, Vol. 16, No. 4:

On p. 177, line 22 from top, read ... $C_R \approx 1/30 C_1 \approx 5C_p$ ... instead of $C_R \approx 1/30$, $C_1 \approx 5C_p$.